Ecological Processes

RESEARCH

Open Access

Effects of altitude and slope on the climate–radial growth relationships of *Larix olgensis* A. Henry in the southern Lesser Khingan Mountains, Northeast China

Jingjing Qiao and Yujun Sun*

Abstract

Background: The relationship between climate and radial growth of trees exhibits spatial variation due to environmental changes. Therefore, elucidation of how the growth–climate responses of trees vary in space is essential for understanding forest growth dynamics to facilitate scientific management with the ongoing global climate warming. To explore the altitudinal and slope variations of these interactions, tree-ring width chronologies of *Larix olgensis* A. Henry were analyzed in the southern Lesser Khingan Mountains, Northeast China.

Results: The radial growth of *L. olgensis* exhibited significant 5- to 10-year periodic changes at three altitudes and two slopes, and the frequency change occurred mainly during the early growth stage and after 2000. The radial growth of *L. olgensis* was significantly negatively correlated with September precipitation only at low altitudes, but also with the mean temperature in July–August and the mean maximum temperature in June–August at high altitudes. The radial growth of *L. olgensis* at low and middle altitudes as well as on the sunny slope led to a higher demand for moisture, while temperature was the key limiting factor at high altitudes and on the shady slope.

Conclusions: The climate–radial growth relationship of *L. olgensis* exhibits altitudinal and slope variability. This study quantitatively describes the spatially varying growth–climate responses of *L. olgensis* in the southern Lesser Khingan Mountains, which provides basic data for the management of *L. olgensis* forests and the prediction of future climate impacts on forest ecosystems.

Keywords: *Larix olgensis* A. Henry, Altitudinal gradient, Slope variability, Lesser Khingan Mountains

Introduction

Global warming has observably affected the environment (IPCC 2014; NASA 2021) and has changed the structure and function of forest ecosystems (Lenoir et al. 2008; Lindner et al. 2010), especially in high latitudes and altitudes in the Northern Hemisphere (Serreze et al. 2000; Andreu et al. 2007; Zhang et al. 2016; Wang et al. 2017). Whether there are stable climate–radial growth relationships of specific tree species has become a scientific issue of wide concern (Babst et al. 2018). Tree ring represents the footprint of tree growth (Ogden 1981; Babst et al. 2018; Silva et al. 2019) and is associated with advantages, such as high annual resolution, accurate age-dating, and wide sample distribution (Douglass 1941; Fritts 1976; He et al. 2019; Silva et al. 2019). Tree rings are one of the essential means to study climate–growth relationships and calculate and predict the variation of forest growth, forest biomass, forest stock volume, and forest carbon

*Correspondence: sunyj@bjfu.edu.cn

National Forestry & Grassland Administration Key Laboratory of Forest Resources & Environmental Management, Beijing Forestry University, Beijing 100083, China

storage at various time scales (Babst et al. 2014, 2018; He et al. 2019; Yu and Liu 2020).

Numerous studies investigating climate–radial growth relationships involve dominant tree species in alpine mountains, arid areas, and other monsoon climate regions (Yu et al. 2006; Shen et al. 2016; Babst et al. 2018; Panthi et al. 2018; He et al. 2019; Jiao et al. 2019). The findings consistently show that the radial growth of trees is significantly affected not only by weather-related environmental factors, but also by regional physiognomic characteristics, especially altitude and slope (Yu et al. 2013; Zhang et al. 2017; Zhu et al. 2018; Yu and Liu 2020). Specifically, growth is mainly affected by precipitation at low altitudes and temperature at high altitudes in Laobai Mountains, Lesser Khingan Mountains, Changbai Mountains, and Hengduan Mountains (Zhu et al. 2018; Sun et al. 2020; Yu and Liu 2020). Temperature was the key limiting factor for tree distribution on different slopes of Changbai Mountains (Chi et al. 1982; Yu et al. 2011, 2013; Yu and Liu 2020). However, these key limiting climatic factors of tree growth are not necessarily applicable for other tree species at various altitudes and slopes in other regions (Yu et al. 2011; Babst et al. 2018; He et al. 2019; Li et al. 2020a, b, c; Zhang et al. 2020a, b, c). Therefore, extensive studies are needed to investigate the spatially varying growth–climate responses of widely distributed forests.

Rapid climate warming has been reported in the middle to high latitudes and high-elevation mountainous regions (Muhlfeld et al. 2011). The Lesser Khingan Mountains are a typical region of climate warming due to its high latitude, where the climate–radial growth relationship of trees exhibits obvious regional characteristics (Shen et al. 2015; Lei et al. 2016). Numerous studies focused on the mixed broad-leaved Korean pine (*Pinus koraiensis* Siebold & Zucc.) forest have shown that the tree growth in this region is affected by temperature and precipitation, especially high temperatures (Yin et al. 2009; Lei et al. 2016; Yu et al. 2017; Li et al. 2020a, b, c). *Larix olgensis* A. Henry is the main afforestation tree species in the region, with a considerable distribution area (Wang et al. 2011; Yu et al. 2017; Li et al. 2020a, b, c). With its substantial forest stock volume and carbon sequestration capacity, this tree species plays a pivotal role in regional and even global carbon and nitrogen cycles and sustainable forest management (Wang et al. 2011; Lei et al. 2016). However, comparatively fewer studies explored its climate–radial growth relationships, with inconsistent results (Andreu et al. 2007; Yin et al. 2009; Lin et al. 2013; Yu et al. 2017; Yu and Liu 2020). Climate warming promoted the radial growth of *L. olgensis* in the Changbai Mountains (Lin et al. 2013). Its radial growth is significantly limited by climate change in Iberian, which showed an upward abrupt at the end of the first half of the twentieth century and a downward shift during the mid-twentieth century (Andreu et al. 2007). Climate warming exerted an inhibitory effect on its radial growth in other areas of Northeast China (Yu and Liu 2020). Therefore, how the radial growth of *L. olgensis* responds to climate change in the Lesser Khingan Mountains, Northeast China requires further exploration.

We hypothesized that the climate–radial growth relationship of *L. olgensis* is strongly regulated by the local climate in our study area. To investigate this hypothesis, we developed a widely distributed tree-ring width chronology to analyze the diverse growth–climate relationships over different altitudes and slopes. Our aims were (a) to elucidate the periodicity patterns of the radial growth of *L. olgensis* at different altitudes and slopes, (b) to detect the growth–climate relationships, and (c) to identify and quantify the climatic factors driving its radial growth. The findings provide first-hand data underlying the dynamic growth of *L. olgensis* and the prediction of forest growth, biomass, stock volume, and carbon storage, which can guide sustainable regional forest management.

Materials and methods

Study area

The study area is located in Dongzhelenghe Nature Reserve in the southern Lesser Khingan Mountains, Northeast China (46° 29′ to 47° 06′ N, 128° 30′ to 129° 24′ E, 200–970 m, Fig. 1a and b). It has a temperate continental monsoon climate with warm rainy summers and long cold winters. The mean annual temperature recorded for the 1966–2018 period at the Yilan Meteorological Station (46° 18′ N, 129° 35′ E, 100.1 m, Fig. 1b) is 3.7 °C, with January being the coldest month (− 22.4 ℃) and July being the warmest (27.5 ℃). The mean annual precipitation is 546.7 mm, approximately 82% of which is deposited in the warm season (May–September). Frost occurs often, and the frost-free period lasts only 90 to 110 days (end of May–beginning of September). Its main forest community type is natural Korean pine and broad-leaved mixed forest. *L. olgensis* and *P. koraiensis* are distributed widely as the dominant coniferous tree species.

Sampling and chronology establishment

The sample cores of *L. olgensis* were collected at five sampling sites in July 2019 (Fig. 1c and Table 1), spanning an elevation of 286–600 m. Sampling sites of different altitudes were set on a sunny slope, and those of different slopes were set at an altitude of approximately 300 m (Table 1). All sample trees were visually assessed before sampling to ensure that only healthy trees in the upper part of the canopy were sampled. To minimize damage to

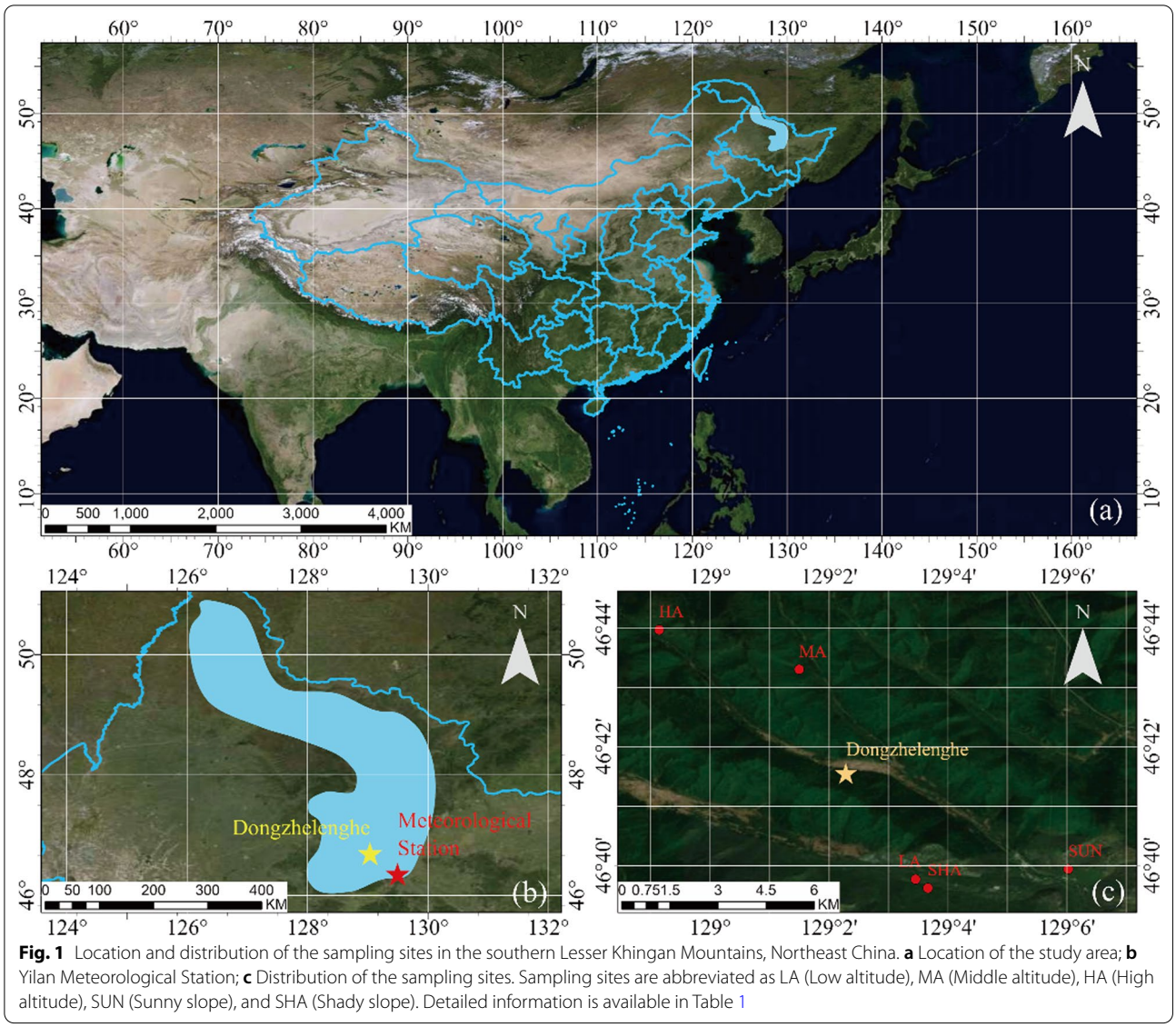

Fig. 1 Location and distribution of the sampling sites in the southern Lesser Khingan Mountains, Northeast China. **a** Location of the study area; **b** Yilan Meteorological Station; **c** Distribution of the sampling sites. Sampling sites are abbreviated as LA (Low altitude), MA (Middle altitude), HA (High altitude), SUN (Sunny slope), and SHA (Shady slope). Detailed information is available in Table 1

Table 1 Information of sampling sites

Sampling site	LA Low altitude	MA Middle altitude	HA High altitude	SUN Sunny slope	SHA Shady slope
Latitude (N)	46° 39′ 46.29″	46° 43′ 17.99″	46° 43′ 58.09″	46° 39′ 56.47″	46° 39′ 37.38″
Longitude (E)	129° 03′ 27.26″	129° 01′ 29.75″	128° 59′ 08.36″	129° 06′ 01.57″	129° 03′ 39.66″
Elevation (m)	286	461	600	305	302
Slope steepness (°)	12	12	13	16	14
Slope aspect (°)	South by east 19	South by east 23	South by east 20	South by east 16	North by east 29
Soil	Dark brown soil	Dark brown soil	Dark brown soil	Dark brown soil	Dark brown soil
Average DBH (mean ± SE, cm)	22.85 ± 0.66	28.05 ± 0.31	28.66 ± 0.79	24.64 ± 0.69	33.10 ± 0.80
Number of total samples (*n*)	95	64	63	83	85
Number of samples for chronology (*n*)	87	60	56	77	65

the trees, only one core was extracted from each tree at diameter at breast height (DBH, 1.3 m above ground). In total, 390 cores were extracted.

The collected core samples were taken back to the laboratory for subsequent processing. The mounted cores were first polished with increasingly finer sandpaper from 100 to 1000 girt until the tree-ring boundaries were clearly visible. They were then visually cross-dated with the skeleton plot method under a Leica-S4E stereo microscope with LINTAB™ 6.0. Forty-five cores with abnormal ring features were excluded from the analysis, such as those with missing rings or indistinct boundaries that made cross-dating difficult (Douglass 1941; Silva et al. 2019). The tree-ring width was measured using a LINTAB™ 6.0 measuring system with an accuracy of 0.01 mm. The quality of measurement and cross-dating was checked using the COFECHA program (Holmes 1983). To remove the effect of non-climatic factors, tree-ring width series were detrended and standardized using the ARSTAN program (Cook and Holmes 1986) with a 67% cubic smoothing spline function at a 50% cutoff frequency. The standard chronologies (STD), the residual chronologies (RES), and the autoregressive chronologies (ARS) in each site were established. Having taken all chronological statistical parameters (Fritts 1976) into account, we focused on STD (Fig. 2) and RES (Fig. 3) for

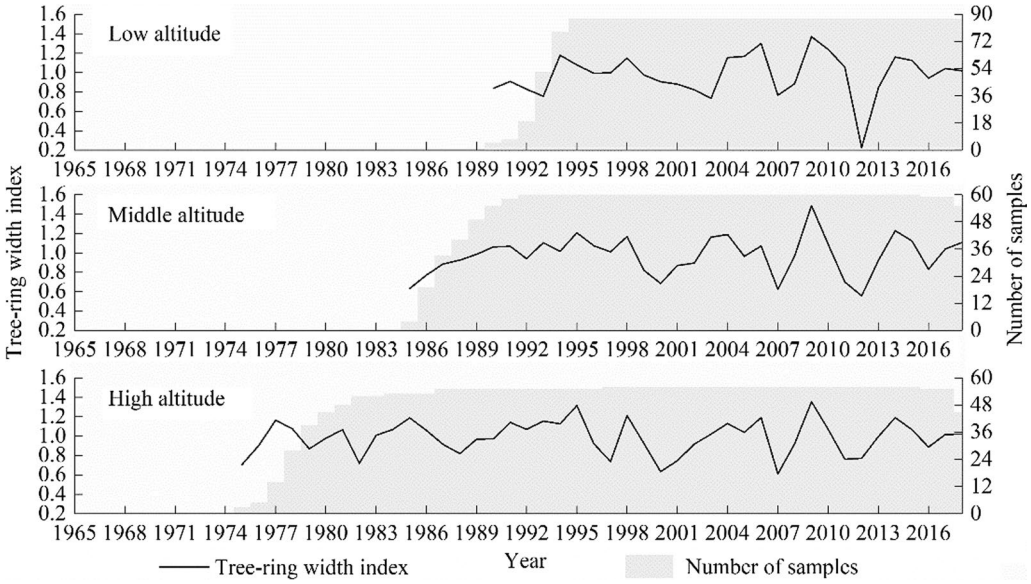

Fig. 2 Tree-ring width standard chronologies (solid black line) with their sample depths (grey-shaded area) along the altitudinal gradient

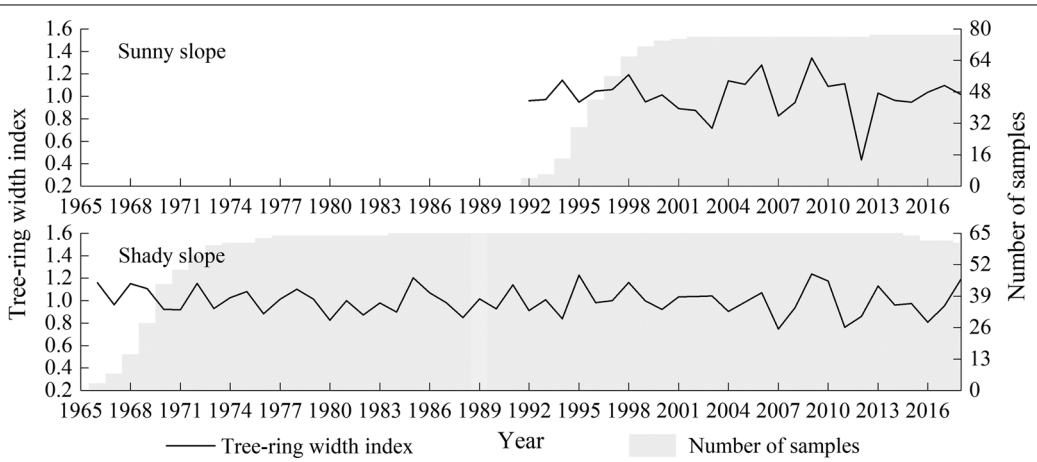

Fig. 3 Tree-ring width residual chronologies (solid black line) and the sample depths (grey-shaded area) at different slopes

the following analysis at different altitudes and slopes, respectively.

Climate data

As the local meteorological stations were far from our sampling sites, the monthly temperature and precipitation of the Climate Research Unit (CRU) TS 4.04 (land) gridded dataset from 1966 to 2018 were utilized for this study. The Palmer Drought Severity Index (PDSI) was used to represent the soil water balance and reflect drought conditions in this study (Mika et al. 2005), which was downloaded from the self-calibrating PDSI Global dataset of the CRU spanning 1966–2017. The above datasets were collected from the Royal Netherlands Meteorological Institute (KNMI) climate explorer (http://climexp.knmi.nl) with a spatial resolution of 0.5° × 0.5°. Considering the growth characteristics of *L. olgensis* and the possible lagged effects of weather conditions on it, the climatic factors from May of the past year to September of the current year were selected for subsequent analysis (Fig. 4).

Statistical analysis

The Mann–Kendall method (Kendall and Gibbons 1992) and wavelet analysis (Addison 2002) were used with MATLAB to analyze the trends and phase mutation of radial growth and its periodic change patterns on multiple time scales, respectively. Radial growth–climate relationships among different altitudes and slopes were determined by response and correlation function analysis with the DendroClim2002 program (Biondi and Waikul 2004). Then, they were further tested by redundancy analysis (RDA) with CANOCO 5.0 software (Ter Braak and Smilauer 2012). The impact of each climatic factor on the radial growth of *L. olgensis* at different altitudes and slopes was quantitatively described by simplified regression equations with R software. Figures were drawn with Origin 16.0.

Results and discussion

Interannual characteristics of climate change

The mean, mean minimum, and mean maximum annual temperature has been rising since 1966 (Fig. 4a–c). The mean minimum temperature has risen almost three times as much as the mean maximum temperature. The precipitation and air relative humidity fluctuated in a small range, with the overall trend decreasing first and increasing slightly subsequently (Fig. 5d and e). The PDSI ranged from −3.36 to 2.67, much of which was less than −2, and its rate of decrease was 0.024 year^{-1} (Fig. 5f). The region showed obvious climate warming and drying, consistent with the overall climate change in Northeast China (Sun et al. 2005; Ye et al. 2019a, b).

With this trend enhanced and its affected areas expanded, more extensive and severe droughts will occur in the land area in the next 30–90 years (Huang et al. 2016; Ye et al. 2019a, b). The adverse effects of drought, such as tree mortality and forest degradation, have been confirmed by some studies (Tang et al. 2015; Jiao et al. 2019). Barber et al. (2000) found reduced growth of Alaskan white spruce from temperature-induced drought stress in most areas of the northern United States. The widespread decline and mortality of trees have also been confirmed in the shelterbelt forests of northern China in recent decades and may become more severe (Li et al. 2020a, b, c). At the same time, the spruce–fir–Korean pine forest would replace *Pinus sylvestris* var. *sylvestriformis* in the community ecotone of the Changbai Mountains under this continuous trend (Yu et al. 2006). Similarly, the current regional climate warming and drying have affected the growth of *L. olgensis*, which can hamper the maintenance of its existing dominant ecological niche.

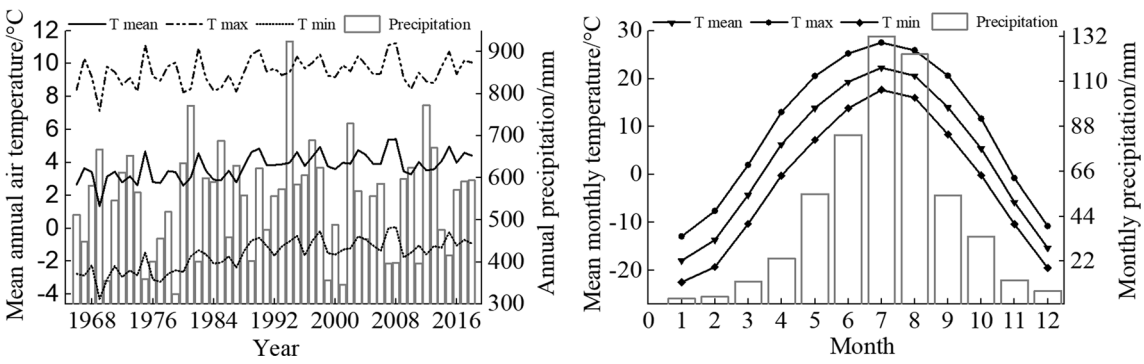

Fig. 4 Interannual (left) and monthly (right) variations of temperatures (mean, maximum, minimum) and precipitation in Dongzhelenghe Nature Reserve from 1966 to 2018

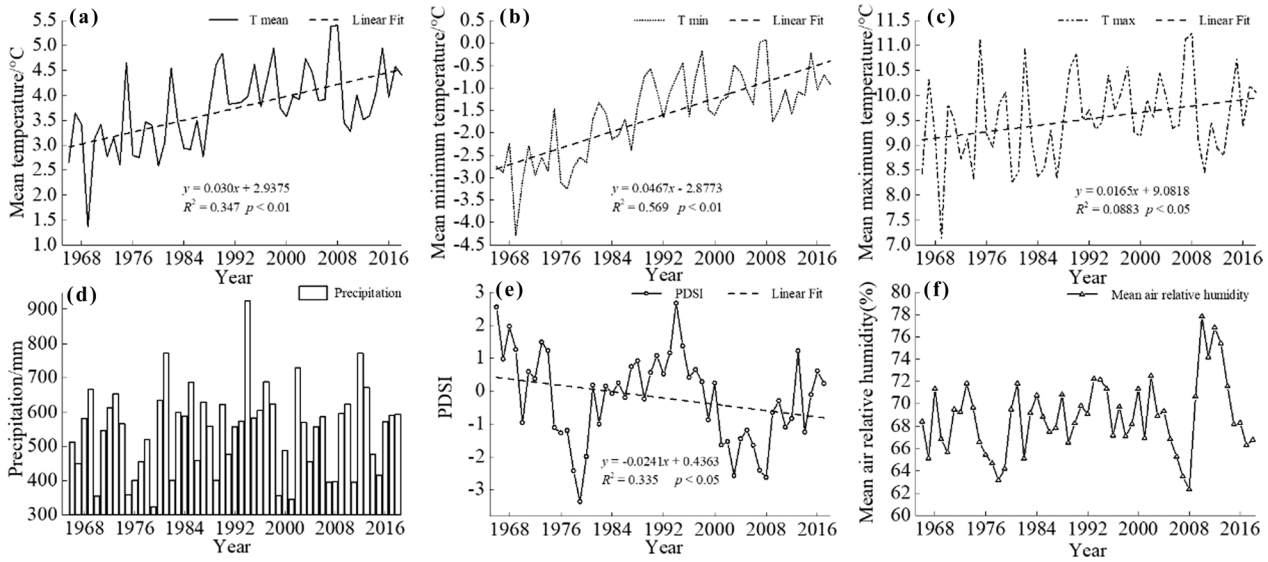

Fig. 5 Climatic interannual changing trend in the study area during the period of 1966–2018. **a** Mean temperature, **b** mean minimum temperature, **c** mean maximum temperature, **d** precipitation, **e** PDSI, and **f** air relative humidity. The dashed lines are indicative of the significant linear regression trends with the equations, *p* values, and R^2 values highlighted

Statistical characteristics of tree-ring width chronologies

There were no significant differences in growth rate among the five chronologies, with a mean growth rate of 0.9894 mm year^{-1} (Table 2). The standard deviations and correlations between trees ranged from 0.12 to 0.22 and 0.30 to 0.71, respectively, which showed that the established chronologies had high regional consistency and could reflect the growth status of *L. olgensis* at different altitudes and slopes. The mean sensitivity varied from 0.15 to 0.23, and the signal-to-noise rate varied from 4.69 to 12.14, indicating that all chronologies retained abundant climatic information. The variation in first eigenvector ranged from 33.5 to 78.1%. The expressed population signal ranged from 0.966 to 0.995, which all exceeded a threshold of 0.85. The chronology statistics are similar to those reported in previous studies for this (Lin et al. 2013; Shen et al. 2016; Yu and Liu, 2020) and other species (Yin et al. 2009; Yu et al. 2017; Li et al. 2020a, b, c). The established chronologies are suitable for climate–growth analyses.

Periodicity of the tree-ring width index

The overall change trends of the tree-ring width index of *L. olgensis* were similar at different altitudes and slopes, with large fluctuations from 2007 to 2012 (Figs. 2 and 3). The minimum value of the tree-ring width index was

Table 2 Statistics of tree-ring width chronologies and common interval analysis

Statistic characters	Standard chronology			Residual chronology	
	Low altitude	Middle altitude	High altitude	Sunny slope	Shady slope
Chronology length (year)	29	34	44	27	53
Mean growth rate (mm year^{-1})	0.9767	0.9771	0.9868	1.0051	1.0012
Common intervals	1992–2018	1987–2018	1979–2017	1992–2018	1969–2017
Mean sensitivity	0.2314	0.1998	0.1918	0.1924	0.1530
Standard deviation	0.2212	0.1989	0.1737	0.1750	0.1202
Correlation between trees	0.707	0.617	0.364	0.540	0.302
First order autocorrelation	0.1614	0.2670	0.1407	-0.0628	-0.1384
Signal-to-noise rate	9.675	9.672	10.864	4.690	12.140
Expressed population signal	0.995	0.989	0.969	0.989	0.966
Variation in first eigenvector (%)	78.1	68.5	41.3	65.6	33.5

detected at high altitudes and on shady slope in 2007 and at other altitudes and sunny slope in 2012, while the maximum value was found in 2009. The severe autumn drought of 2007, the low temperature and heavy summer rainfall of 2012, and the *Dendrolimus superans* infestation in some areas during this time adversely affected the growth of *L. olgensis* (Li et al. 2016; Liang et al. 2018), which was reflected in periodic change in its radial growth.

A statistically significant decrease or increase in tree-ring width index was observed in the early growth stage and after 2000, despite the absence of precise mutation year (Fig. 6). The rapid warming in Northeast China after 2000 may have contributed to these results (Zhou et al. 2020). In addition, during the early growth stage, the roots of trees grow relatively slowly and exhibit poor water use efficiency, making trees more sensitive to hydrothermal conditions, resulting in significant fluctuation in radial growth (Schenk and Jackson 2002; Rozas et al. 2009; Brunner et al. 2015). Relevant studies also proved that trees in the early growth stage are more sensitive to climatic factors, such as *Quercus rubra* L. in the northern USA, Smith fir (*Abies forrestii* var. *smithii* R. Vig. & Gaussen) in the northeast Tibetan Plateau, black spruce (*Picea mariana* [Mill.] Britton, Sterns & Poggenb.) in the semi-humid climate region of Manitoba, and *Juniperus thurifera* L. in the semi-humid climate region of north-central Spain (McMillan et al. 2008; Rozas et al. 2009; Haavik et al. 2011; Li et al. 2013).

The tree-ring width index of *L. olgensis* showed significant 5- to 10-year periodic variations at various altitudes and slopes during different periods. It was 2003–2018, 2004–2017, and 1996–2018 with the altitude increased and 2002–2018 and 2009–2018 on the sunny slope and shady slope, respectively (Fig. 7). These may be related to large-scale climate change and non-climatic pressures, such as global climatic oscillation and land–sea thermal differences (Piraino and Roig 2013; Venegas-González et al. 2015; Zhu et al. 2017; Yu et al. 2021). Similar results were reported in the Changbai Mountains, Qinling Mountains, and Tianshan Mountains, indicating a universal impact of large-scale climate on tree growth (Yu et al. 2018, 2021; Jiang et al. 2019; Jiao et al. 2019).

Growth–climate relationships

Altitudinal variability of the growth–climate relationships

The radial growth of *L. olgensis* at various altitudes was mainly affected by the climatic factors of the current year (Fig. 8). The impact of temperature increased, while precipitation decreased with increasing altitude (Figs. 8, 9a). Similar studies conducted in Northeast China (including Changbai Mountains), Qilian Mountains, and Hengduan Mountains reported the same conclusions (Zhang et al. 2017; Zhu et al. 2018; Sun et al. 2020; Yu and Liu, 2020).

Temperatures and hydrothermal conditions in summer play a critical role in the radial growth of *L. olgensis* at high altitudes (Fig. 8). Specifically, the radial growth was significantly negatively correlated with the current

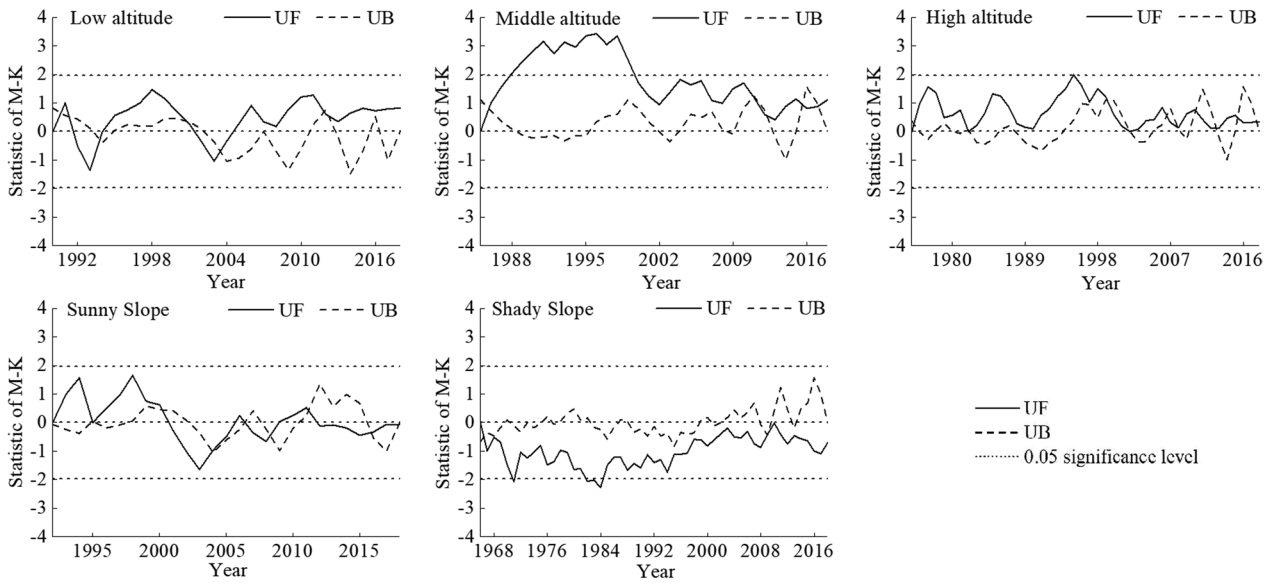

Fig. 6 Mann–Kendall mutation test curves of tree-ring width index with forward statistic UF (solid line) and backward statistic UB (dashed line) at the 0.05 significance level (dotted horizontal lines). The intersection of the UF and UB curves is located between the critical lines, corresponding to the time the mutation begins

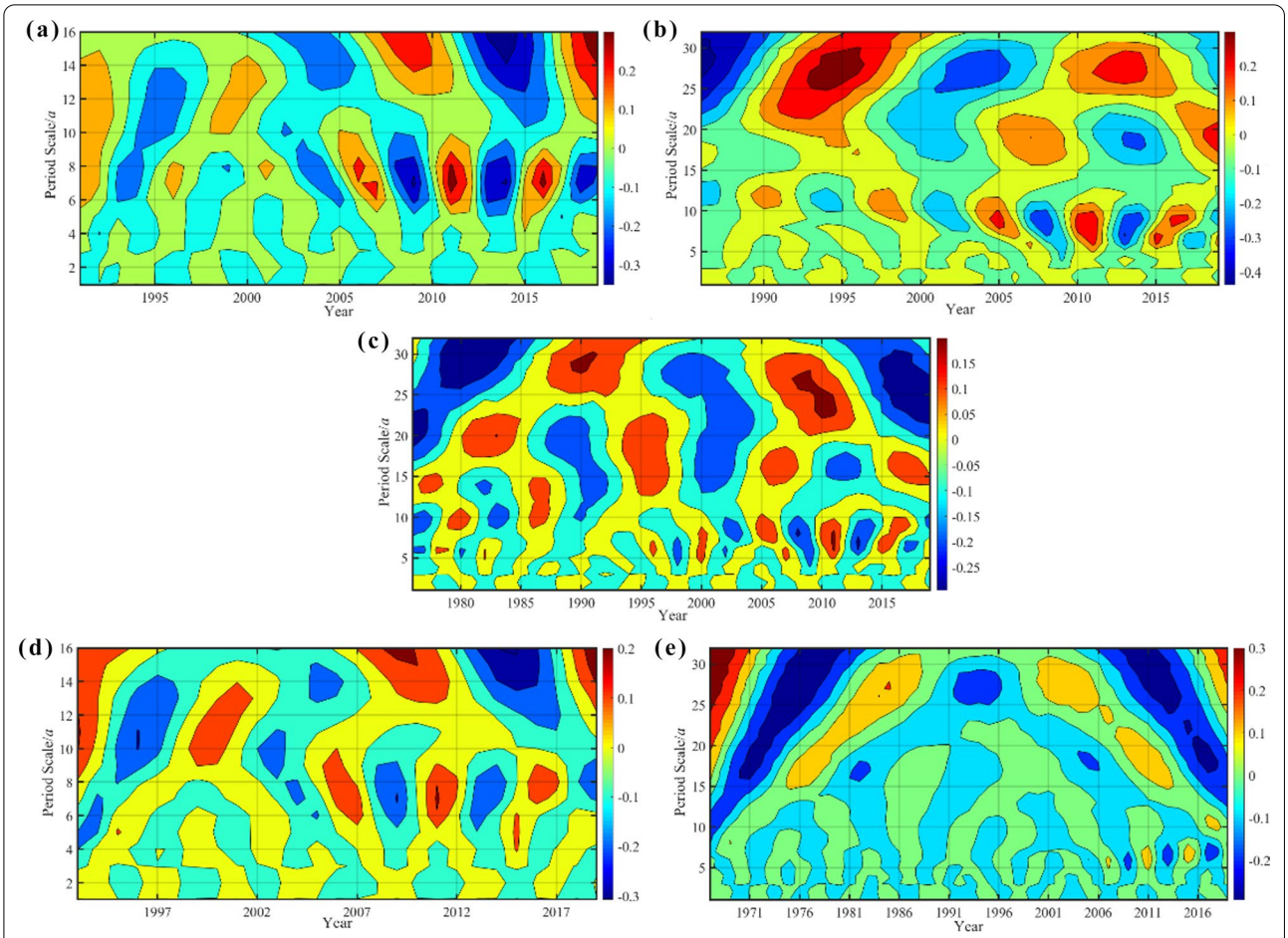

Fig. 7 Real part wavelet coefficient contour map of tree-ring width index at **a** low altitude, **b** middle altitude, **c** high altitude, **d** sunny slope, and **e** shady slope. *Y*-axis is the scale in year, and *X*-axis is the time in year

July–August T_{mean} ($r=-0.359$, $r=-0.313$) and the current June–August T_{max} ($r=-0.317$, $r=-0.446$, $r=-0.310$) and significantly positively correlated with the current July PDSI ($r=0.361$) and the current June–July RH ($r=0.434$, $r=0.516$). Summer is the peak growing season of *L. olgensis* (Wang et al. 2011). Nevertheless, excessively high temperatures decrease moisture in the atmosphere and soil, adversely affecting its growth by disrupting its basic metabolic balance (Will et al. 2013; Zhang et al. 2020a, b, c). Similar studies involving *Pinus armandii* Franch. in Qinling Mountains, *Picea abies* (L.) H. Karst. in the central part of the Ceskomoravska Upland, and four dominant conifer species in western Labrador, Canada, showed that high temperatures in summer led to the formation of narrow rings (Nishimura and Laroque 2011; Rybnícek et al. 2012; Wang et al. 2016).

The adverse effects of current September precipitation on radial growth were intensified with decreasing altitude, which showed a significant negative correlation at low altitudes ($r=-0.484$), a slight negative correlation at middle altitudes ($r=-0.252$), and no correlation at high altitudes ($r=-0.054$) (Figs. 8, 9a). This is consistent with the results of studies investigating the radial growth response to climate in major conifers on Haba Snow Mountain in Southwest China and areas in southern Europe (Caminero et al. 2018; Zhang et al. 2020a, b, c). Temperature decreases rapidly in September (Fig. 9), and the first snowfall and frost will advance if precipitation continues to increase at this time, which increases the risk of chilling and freezing injury to trees (Horimoto and Araki 1999). At the same time, this weather does not facilitate nutrient accumulation and lignification in trees by regulating the activities of soil microorganisms related to the emission and absorption of carbon dioxide (CO_2) and methane (CH_4) (Bukata and Kyser 2007; Bhattacharyya et al. 2013; Wagner et al. 2016; Praeg et al. 2017), which shortens the growing season and prematurely terminate their radial growth (Babst et al. 2014).

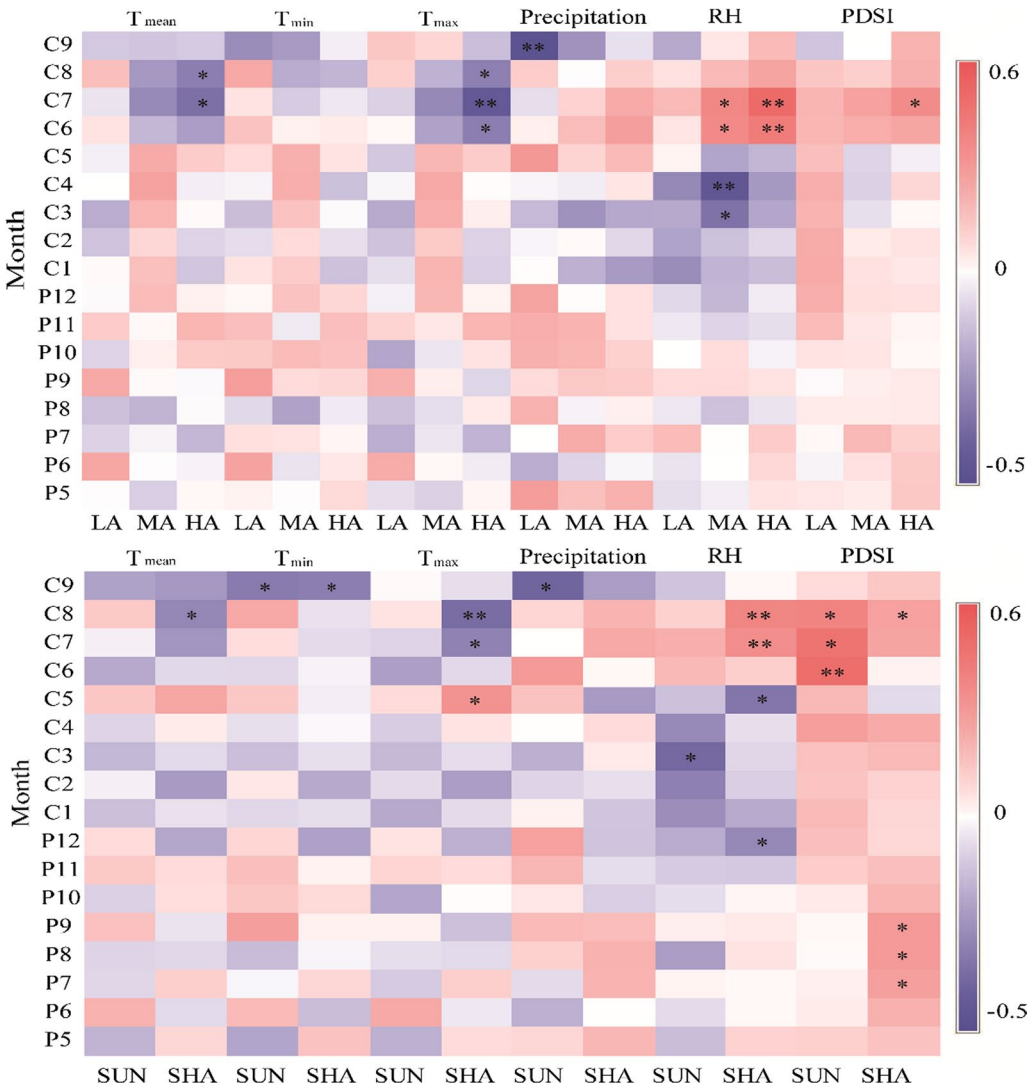

Fig. 8 Response of radial growth of *L. olgensis* to monthly climatic factors at different altitudes (the upper half) and slopes (the lower half). The capitalized P means months from the past year and C from the current year. The gradual change of color from blue to red indicates a gradual change of correlation from negative to positive. *$p < 0.05$; **$p < 0.01$

Nevertheless, the results of this study differ from those associated with the radial growth response of *L. olgensis* to climate in the Changbai Mountains and *Picea crassifolia* Kom. in Qilian Mountains (Yu and Liu, 2020; Zhang et al. 2020a, b, c). The possible reasons are as follows: first, the study areas, located in different climatic provinces, exhibit distinct climate variation; second, regional differences lead to different phenological characteristics and growth rhythm of trees; and third, the differences in the microenvironment of the sampling sites may also contribute to these differences.

Slope variability of the growth–climate relationships

The radial growth of *L. olgensis* was mainly limited by temperature on the shady slope but by the moisture conditions of soil and air on the sunny slope (Figs. 8, 9b). Specifically, on the shady slope, it was significantly negatively correlated with the current August T_{mean} ($r = -0.288$), the current September T_{min} ($r = -0.315$), the current July–August T_{max} ($r = -0.300$, $r = -0.370$), and the current May and previous December RH ($r = -0.343$, $r = -0.282$). It had a significantly positive correlation with the current May T_{max} ($r = 0.332$), the current

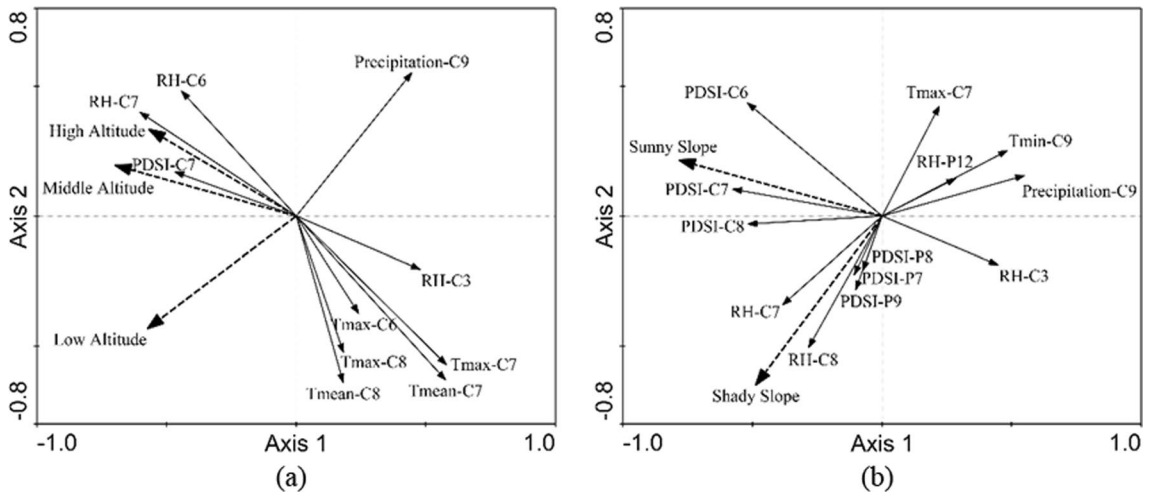

Fig. 9 Redundancy analysis (RDA) for the chronologies and the monthly climatic factors at different altitudes (**a**) and slopes (**b**). Significant ($p < 0.05$) climatic factors are indicated by solid line arrows and named as "the climatic factor-corresponding month" (e.g., the mean temperature in July of the current year named as Tmean-C7). Arrow (vector) length and the cosine of the angle between two vectors depict the magnitude of variables and their correlation. The longer the vector, the more important the climatic factor. Vectors crossing at sharp angles, obtuse angles, and right angles, respectively, indicate a positive correlation, a negative correlation, and a near-zero correlation

July–August RH ($r=0.356$, $r=0.394$), and the current August and previous July–September PDSI ($r=0.274$, $r=0.279$, $r=0.299$, $r=0.305$). Because of the shorter duration and weaker intensity of direct solar radiation on the shady slope (Chi et al. 1982), tree growth increases the demand on temperature, particularly at the beginning of and the growing season. Temperature increases in May during the start of *L. olgensis* growth in this region (Ogden 1981; Wang et al. 2011; Silva et al. 2019), accelerating the metabolic activities of soil microorganisms such as methanotrophs (Praeg et al. 2017) and promoting carbon and nitrogen cycles of the ecosystem (Bukata and Kyser 2007; Bhattacharyya et al. 2013; Babst et al. 2014), which contributes to the accumulation of organic matter in plants (Wagner et al. 2016), thus facilitating the radial growth of trees. Studies on the growth–climate relationships of *Larix decidua* Mill. in the French Alps, *Abies georgei* Hand.-Mazz. in Haba Snow Mountain, and the southern part of the Asian boreal forests in Northeast China also corroborated our results (Saulnier et al. 2019; Li et al. 2020a, b, c; Zhang et al. 2020a, b, c).

The PDSI in current June had the strongest impact on the radial growth of *L. olgensis* on sunny slope, followed by the current March air relative humidity (Figs. 8, 9b). The correlation between the two was positive ($r=0.500$) and negative ($r=-0.386$), respectively. The results are consistent with those of other relevant studies, in which moisture availability was a major limiting factor for pine forests in Southwest and Northeast China (Zhu et al. 2018; Bi et al. 2020). In March, the mean temperature is still below 0 ℃ in the southern Lesser Khingan Mountains (Fig. 9), when trees are more vulnerable to freezing injury under increased air relative humidity (Horimoto and Araki, 1999). Further, the high temperature in June–August leads to high water evaporation; therefore, trees on the sunny slope benefit from the increased soil moisture (Kim et al. 2011). Studies on the northern and eastern slopes of the Changbai Mountains also established the slope variability of the growth–climate relationships (Yu et al. 2011, 2013; Yu and Liu, 2020).

Simulation of growth–climate relationships

No multicollinearity was found among the explanatory variables, and the statistical characteristics (R^2 and p-values) of the established models were generally high (Table 3). Temperature had the strongest limiting effect at high altitudes, with an explanation rate of 48.95%. Moisture was the main limiting factor for the radial growth of *L. olgensis* at low and middle altitudes, accounting for 72.71% and 94.92%, respectively. In addition, temperature had a high limiting effect on the radial growth of *L. olgensis* on the shady slope (with the explanation rate of 47.60%), while moisture had a high explanation rate of 76.89% on the sunny slope. The established models fit the objective law of the influence of climate factors on the radial growth of *L. olgensis* and prove the altitude and slope variability in radial growth–climate relationships.

Differences in radial growth response to climatic factors cannot be explained merely by geographic location, growth characteristics, microenvironment, and spatial

Table 3 Optimal simplified multiple regression model for growth-climate of *L. olgensis*

	Optimal simplified multiple regression equation	R^2	*p*-value
Low altitude	$Y = 0.330 \times A_8 - 0.531 \times J_9 + 0.349 \times R_7$	0.382	0.0080
Middle altitude	$Y = -0.067 \times A_7 - 0.284 \times J_9 - 0.460 \times R_4 + 0.227 \times R_6 + 0.285 \times R_7$	0.490	0.0020
High altitude	$Y = -0.122 \times A_7 - 0.116 \times H_6 - 0.179 \times H_8 + 0.110 \times P_7 + 0.325 \times R_7$	0.346	0.0060
Sunny slope	$Y = 0.469 \times A_8 - 0.402 \times J_9 + 0.285 \times P_6 - 0.436 \times R_3 + 0.439 \times R_7$	0.639	0.0006
Shady slope	$Y = -0.146 \times A_8 - 0.090 \times L_9 + 0.267 \times H_5 - 0.155 \times H_7 - 0.230 \times J_9 + 0.303 \times PP_8 + 0.192 \times R_7$	0.413	0.0009

A_i mean temperature of the month *i* of the current year; J_i precipitation of the month *i* of the current year; R_i air relative humidity of the month *i* of the current year; H_i mean maximum temperature of the month *i* of the current year; P_i PDSI of the month *i* of the current year; L_i mean minimum temperature of the month *i* of the current year; PP_i PDSI of the month *i* of the past year

competition. Large-scale climate phenomena, such as global climatic oscillation and land–sea thermal differences, global carbon and nitrogen cycles, and non-climatic pressures also contribute to the differences (Bukata and Kyser 2007; Bhattacharyya et al. 2013; Piraino and Roig 2013; Babst et al. 2014; Venegas-González et al. 2015; Zhu et al. 2017; Yu et al. 2021). Admittedly, our study is only based on *L. olgensis* in the region and does not cover long-term climate change on a large scale. Therefore, further studies of climate–radial growth relationships with a more extensive and intensive sampling of multiple species are critically important. These efforts will better understand the applicability of current laws and provide a theoretical basis for estimating the carbon stock and sequestration and management of *L. olgensis* forests, such as afforestation and harvesting.

Conclusions

The radial growth of *L. olgensis* in the southern Lesser Khingan Mountains shows obvious 5- to 10-year periodicity. The temporal instability mainly occurred in the early growth stage and after 2000. The growth–climate response exhibits distinct altitudinal and slope variability. The radial growth of *L. olgensis* at low altitudes is mainly affected by precipitation, but also by temperature, especially the high temperature in summer at high altitudes. Temperature is the key climate limiting factor for the distribution of *L. olgensis* on shady slope. Future climate changes will exacerbate the challenges underlying the adaptive growth of *L. olgensis* in this region.

Abbreviations

LA: Low altitude; MA: Middle altitude; HA: High altitude; SUN: Sunny slope; SHA: Shady slope; DBH: Diameter at breast height; STD: The standard chronology; RES: The residual chronology; ARS: The autoregressive chronology; CRU : Climate Research Unit; PDSI: The Palmer Drought Severity Index; KNMI: Royal Netherlands Meteorological Institute; RDA: Redundancy analysis; T_{mean}: Mean temperature; T_{max}: Mean maximum temperature; T_{min}: Mean minimum temperature; RH: Air relative humidity; UF: Forward statistic; UB: Backward statistic; P: Past year; C: Current year; A_i: Mean temperature of the month *i* of the current year; J_i: Precipitation of the month *i* of the current year; R_i: Air relative humidity of the month *i* of the current year; H_i: Mean maximum temperature of the month *i* of the current year; P_i: PDSI of the month *i* of the current year; L_i: Mean minimum temperature of the month *i* of the current year; PP_i: PDSI of the month *i* of the past year.

Acknowledgements

The authors would like to thank Tong Wang, Lei Pan, Peiwu Han, Xiaojuan Jin and Siyu Qiu for their contributions in collecting field samples. We would like to be grateful to the handing editor and anonymous reviewers for their valuable comments.

Author contributions

JQ and YS designed the study. JQ conducted the field and laboratory analyses. Data analysis was conducted by JQ. The paper was written by JQ with input from YS. All authors read and approved the final manuscript.

Funding

The work was supported by the National Natural Science Foundation of China (Grant No. 31870620) and the Fundamental Research Funds for the Central Universities (Grant No. PTYX202107).

Availability of data and materials

Data of the current study are available from the corresponding author on reasonable request.

Declarations

Ethics approval and consent to participate

Not applicable.

Consent for publication

All authors agreed and approved the manuscript for publication in ***Ecological Processes***.

Competing interests

The authors declare that they have no competing interests.

Received: 26 October 2021 Accepted: 16 June 2022
Published online: 05 July 2022

References

Addison P (2002) The illustrated wavelet transform handbook. CRC Press, Bristol

Andreu L, Gutierrez E, Macias M, Ribas M, Bosch O, Camarero JJ (2007) Climate increases regional tree-growth variability in Iberian pine forests. Global Change Biol 13:804–815. https://doi.org/10.1111/j.1365-2486.2007.01322.x

Babst F, Alexander MR, Szejner P et al (2014) A tree-ring perspective on the terrestrial carbon cycle. Oecologia 176(2):307–322. https://doi.org/10.1007/s00442-014-3031-6

Babst F, Bodesheim P, Charney N, Friend AD, Girardin MP, Klesse S, Moore DJP, Seftigen K, Björklund J, Bouriaud O (2018) When tree rings go global:

challenges and opportunities for retro-and prospective insight. Quat Sci Rev 197:1–20. https://doi.org/10.1016/j.quascirev.2018.07.009
Barber VA, Juday GP, Finney BP (2000) Reduced growth of Alaskan white spruce in the twentieth century from temperature-induced drought stress. Nature 405:668–673. https://doi.org/10.1038/35015049
Bhattacharyya P, Roy KS, Neogi S et al (2013) Impact of elevated CO_2 and temperature on soil C and N dynamics in relation to CH_4 and N_2O emissions from tropical flooded rice (*Oryza sativa* L.). Sci Total Environ 461:601–611. https://doi.org/10.1016/j.scitotenv.2013.05.035
Bi YF, Whitney C, Li JW, Yang JC, Yang XF (2020) Spring moisture availability is the major limitation for pine forest productivity in Southwest China. Forests 11:446. https://doi.org/10.3390/f11040446
Biondi F, Waikul K (2004) DENDROCLIM2002: a C++ program for statistical calibration of climate signals in tree-ring chronologies. Comput Geosci 30:303–311. https://doi.org/10.1016/j.cageo.2003.11.004
Brunner I, Herzog C, Dawes MA, Arend M, Sperisen C (2015) How tree roots respond to drought. Front Plant Sci 6:547. https://doi.org/10.3389/fpls.2015.00547
Bukata AR, Kyser TK (2007) Carbon and nitrogen isotope variations in tree-rings as records of perturbations in regional carbon and nitrogen cycles. Environ Sci Technol 41(4):1331–1338. https://doi.org/10.1021/es061414g
Caminero L, Génova M, Camarero JJ, Sánchez-Salguero R (2018) Growth responses to climate and drought at the southernmost European limit of Mediterranean *Pinus pinaster* forests. Dendrochronologia 48:20–29. https://doi.org/10.1016/j.dendro.2018.01.006
Chi ZW, Zhang FS, Li XY (1982) The primary study on water-heat conditions of forest ecosystem on northern slope of Changbai Mountain. For Ecosyst Res 2:167–178
Cook ER, Holmes RL (1986) Users manual for program ARSTAN. Laboratory of Tree-Ring Research, University of Arizona, Tucson, USA
Douglass AE (1941) Crossdating in dendrochronology. J For 39:825–831. https://doi.org/10.1093/jof/39.10.825
Fritts HC (1976) Tree ring and climate. Academic Press, London
Haavik LJ, Stahle DW, Stephen FM (2011) Temporal aspects of *Quercus rubra* decline and relationship to climate in the Ozark and Ouachita Mountains, Arkansas. Can J For Res 41:773–781. https://doi.org/10.1139/x11-018
He MH, Yang B, Bräuning A, Rossi S, Ljungqvist FC, Shishov V, Grießinger J, Wang JL, Liu JJ, Qin C (2019) Recent advances in dendroclimatology in China. Earth-Sci Rev 194:521–535. https://doi.org/10.1016/j.earscirev.2019.02.012
Holmes RL (1983) Computer-assisted quality control in tree-ring dating and measurement. Tree-Ring Bull 43:69–75
Horimoto M, Araki H (1999) Freezing injury of Japanese chestnut (*Castanea crenata* Sieb. et Zucc.) in relation to changes in twig water content and xylem pressure from winter to early spring. J Agric Meteorol 55:25–32. https://doi.org/10.2480/agrmet.55.25
Huang JP, Yu HP, Guan XD, Wang GY, Guo RX (2016) Accelerated dryland expansion under climate change. Nat Clim Change 6:166–171. https://doi.org/10.1038/NCLIMATE2837
Intergovernmental Panel on Climate Change (IPCC) (2014) Climate Change 2014: Synthesis Report. Contribution of Working Groups I, II and III to the Fifth Assessment Report of the Intergovernmental Panel on Climate Change. Geneva, Switzerland
Jiang YG, Yuan X, Zhang JH, Han SJ, Chen ZJ, Wang XG, Wang JW, Hao L, Li GD, Dong SZ (2019) Reconstruction of June–July temperatures based on a 233 year tree-ring of *Picea jezoensis* var. *microsperma*. Forests 10:416. https://doi.org/10.3390/f10050416
Jiao L, Jiang Y, Zhang WT, Wang MC, Wang SJ, Liu XR (2019) Assessing the stability of radial growth responses to climate change by two dominant conifer trees species in the Tianshan Mountains, northwest China. For Ecol Manage 433:667–677. https://doi.org/10.1016/j.foreco.2018.11.046
Kendall MG, Gibbons JD (1992) Rank correlation methods, 5th edn. Arnold Press, London, p 249
Kim S, Han S, Kim E (2011) Stochastic modelling of soil water and plant water stress using cumulant expansion theory. Ecohydrology 4:94–105. https://doi.org/10.1002/eco.127
Lei XD, Yu L, Hong LX (2016) Climate-sensitive integrated stand growth model (CS-ISGM) of Changbai larch (*Larix olgensis*) plantations. For Ecol Manage 376:265–275. https://doi.org/10.1016/j.foreco.2016.06.024
Lenoir J, Gégout JC, Marquet PA, De Ruffray P, Brisse H (2008) A significant upward shift in plant species optimum elevation during the 20th century. Science 320:1768–1771. https://doi.org/10.1126/science.1156831
Li XX, Liang EY, Gričar J, Prislan P, Rossi S, Čufar K (2013) Age dependence of xylogenesis and its climatic sensitivity in Smith fir on the south-eastern Tibetan Plateau. Tree Physiol 33:48–56. https://doi.org/10.1093/treephys/tps113
Li YS, Duan CF, Wang Y (2016) Evaluation of forecast skill of monthly rainfall over Northeast China using multi-models. J Meteorol Environ 32:61–66. https://doi.org/10.3969/j.issn.1673-503X.2016.05.009
Li M, Fang L, Duan C, Cao Y, Yin H, Ning Q, Hao G (2020a) Greater risk of hydraulic failure due to increased drought threatens pine plantations in Horqin Sandy Land of northern China. For Ecol Manage 461:117980. https://doi.org/10.1016/j.foreco.2020.117980
Li MQ, Deng GF, Shao XM, Yin ZY (2020b) Precipitation reconstruction based on tree-ring width over the past 270 years in the central Lesser Khingan Mountains, Northeast China. Clim Past 56:1–35. https://doi.org/10.5194/cp-2020-56
Li WQ, Jiang Y, Dong MY, Du EZ, Zhou ZJ, Zhao SD, Xu H (2020c) Diverse responses of radial growth to climate across the southern part of the Asian boreal forests in northeast China. For Ecol Manage 458:117759. https://doi.org/10.1016/j.foreco.2019.117759
Liang F, Liu DD, Xu HM, Sun JJ, Feng XF, Mu WF (2018) Comparison of drought variation in Northeast China from 1961 to 2009 by using three drought index datasets. Res Soil Water Conserv 25:183–189. https://doi.org/10.13869/j.cnki.rswc.2018.01.030
Lin B, Xu QQ, Liu WH, Zhang GC, Xu QY, Liu QJ (2013) Dendrochronology-based stand growth estimation of *Larix olgensis* forest in relation with climate on the eastern slope of Changbai Mountain, NE China. Front Earth Sci 7:429–438. https://doi.org/10.1007/s11707-013-0401-z
Lindner M, Maroschek M, Netherer S, Kremer A, Barbati A, Garcia-Gonzalo J, Seidl R, Delzon S, Corona P, Kolström M (2010) Climate change impacts, adaptive capacity, and vulnerability of European forest ecosystems. For Ecol Manage 259:698–709. https://doi.org/10.1016/j.foreco.2009.09.023
McMillan AM, Winston GC, Goulden ML (2008) Age-dependent response of boreal forest to temperature and rainfall variability. Global Change Biol 14:1904–1916. https://doi.org/10.1111/j.1365-2486.2008.01614.x
Mika J, Horvath SZ, Makra L, Dunkel Z (2005) The Palmer Drought Severity Index (PDSI) as an indicator of soil moisture. Phys Chem Earth 30:223–230. https://doi.org/10.1016/j.pce.2004.08.036
Muhlfeld CC, Giersch JJ, Hauer FR, Pederson GT, Luikart G, Peterson DP, Downs CC, Fagre DB (2011) Climate change links fate of glaciers and an endemic alpine invertebrate. Clim Change 106(2):337–345. https://doi.org/10.1007/s10584-011-0057-1
National Aeronautics and Space Administration (NASA) (2021) World of Change: Global Temperatures. https://earthobservatory.nasa.gov/world-of-change/global-temperatures. accessed 28 Feb 2021
Nishimura PH, Laroque CP (2011) Observed continentality in radial growth-climate relationships in a twelve site network in western Labrador, Canada. Dendrochronologia 29:17–23. https://doi.org/10.1016/j.dendro.2010.08.003
Ogden J (1981) Dendrochronological studies and the determination of tree ages in the Australian tropics. J Biogeogr 8(5):405–420. https://doi.org/10.2307/2844759
Panthi S, Bräuning A, Zhou ZK, Fan ZX (2018) Growth response of *Abies georgei* to climate increases with elevation in the central Hengduan Mountains, southwestern China. Dendrochronologia 47:1–9. https://doi.org/10.1016/j.dendro.2017.11.001
Piraino S, Roig FA (2013) North Atlantic oscillation influences on radial growth of *Pinus pinea* on the Italian mid-Tyrrhenian coast. Plant Biosyst 148(2):279–287. https://doi.org/10.1080/11263504.2013.770806
Praeg N, Wagner AO, Illmer P (2017) Plant species, temperature, and bedrock affect net methane flux out of grassland and forest soils. Plant Soil 410(1):193–206. https://doi.org/10.1007/s11104-016-2993-z
Rozas V, DeSoto L, Olano JM (2009) Sex-specific, age-dependent sensitivity of tree-ring growth to climate in the dioecious tree *Juniperus thurifera*. New Phytol 182:687–697. https://doi.org/10.1111/j.1469-8137.2009.02770.x
Rybnícek M, Cermák P, Zid T, Kolar T (2012) Growth responses of *Picea abies* to climate in the central part of the Ceskomoravská Upland (Czech Republic). Dendrobiology 68:21–30. https://doi.org/10.2478/s13386-012-0003-7

Saulnier M, Corona C, Stoffel M, Guibal F, Edouard JL (2019) Climate-growth relationships in a *Larix decidua* Mill. network in the French Alps. Sci Total Environ 664:554–566. https://doi.org/10.1016/j.scitotenv.2019.01.404
Schenk HJ, Jackson RB (2002) Rooting depths, lateral root spreads and below-ground/above-ground allometries of plants in water-limited ecosystems. J Ecol 90:480–494. https://doi.org/10.1046/j.1365-2745.2002.00682.x
Serreze MC, Walsh JE, Chapin FS, Osterkamp T, Dyurgerov M, Romanovsky V, Oechel WC, Morison J, Zhang T, Barry RG (2000) Observational evidence of recent change in the northern high-latitude environment. Clim Change 46:159–207
Shen C, Lei X, Liu H, Wang L, Liang W (2015) Potential impacts of regional climate change on site productivity of *Larix olgensis* plantations in north-east China. iForest 8:642. https://doi.org/10.3832/ifor1203-007
Shen C, Wang L, Li M (2016) The altitudinal variability and temporal instability of the climate–tree-ring growth relationships for Changbai larch (*Larix olgensis* Henry) in the Changbai mountains area, Jilin, Northeastern China. Trees 30:901–912. https://doi.org/10.1007/s00468-015-1330-0
Silva MS, Funch LS, da Silva LB (2019) The growth ring concept: seeking a broader and unambiguous approach covering tropical species. Biol Rev 94(1):1–16. https://doi.org/10.1111/brv.12495
Sun FH, Yang SY, Chen PS (2005) Climatic warming-drying trend in Northeastern China during the last 44 years and its effects. Chin J Ecol 24:751–755
Sun L, Cai Y, Zhou Y, Shi S, Zhao Y, Gunnarson BE, Jaramillo F (2020) Radial growth responses to climate of *Pinus yunnanensis* at low elevations of the Hengduan mountains, China. Forests 11:1066. https://doi.org/10.3390/f11101066
Tang H, Li Z, Zhu Z, Chen B, Zhang B, Xin X (2015) Variability and climate change trend in vegetation phenology of recent decades in the Greater Khingan Mountain area, Northeastern China. Remote Sens 7:11914–11932. https://doi.org/10.3390/rs70911914
Ter Braak CJF, Smilauer P (2012) Canoco reference manual and user's guide: software for ordination, version 5.0. Microcomputer Power, Ithaca
Venegas-González A, Chagas MP, Anholetto Júnior CR, Alvares CA, Roig FA, Tomazello Filho M (2015) Sensitivity of tree ring growth to local and large-scale climate variability in a region of Southeastern Brazil. Theor Appl Climatol 123(1–2):233–245. https://doi.org/10.1007/s00704-014-1351-4
Wagner FH, Hérault B, Bonal D, Stahl C, Anderson LO, Baker TR et al (2016) Climate seasonality limits leaf carbon assimilation and wood productivity in tropical forests. Biogeosciences 13(8):2537–2562. https://doi.org/10.5194/bg-13-2537-2016
Wang XY, Sun YJ, Ma W (2011) Biomass and carbon storage distribution of different density in *Larix olgensis* plantation. J Fujian Coll For 31:221–226. https://doi.org/10.13324/j.cnki.jfcf.2011.03.013
Wang H, Wu J, Sun B, Zhang D, Liu S (2016) Response of radial growth of *Pinus armandii* to climate change in the Qinling mountains. Nat Environ Pollut Technol 15:903–909
Wang X, Zhang M, Ji Y, Li Z, Li M, Zhang Y (2017) Temperature signals in tree-ring width and divergent growth of Korean pine response to recent climate warming in northeast Asia. Trees 31:415–427. https://doi.org/10.1007/s00468-015-1341-x
Will RE, Wilson SM, Zou CB, Hennessey TC (2013) Increased vapor pressure deficit due to higher temperature leads to greater transpiration and faster mortality during drought for tree seedlings common to the forest-grassland ecotone. New Phytol 200:366–374. https://doi.org/10.1111/nph.12321
Ye L, Shi K, Xin Z, Wang C, Zhang C (2019a) Compound droughts and heat waves in China. Sustainability 11:3270. https://doi.org/10.3390/su11123270
Ye L, Shi K, Zhang H, Xin Z, Hu J, Zhang C (2019b) Spatio-temporal analysis of drought indicated by SPEI over northeastern China. Water 11:908. https://doi.org/10.3390/w11050908
Yin H, Liu HB, Guo PW (2009) An analysis on the climatic response mechanism of the growth of *Pinus koraiensis* in the lower mountains of XiaoXing' AnLing. Acta Ecol Sin 2:5–14
Yu J, Liu QJ (2020) *Larix olgensis* growth-climate response between lower and upper elevation limits: an intensive study along the eastern slope of the Changbai Mountains, northeastern China. J For Res 31:231–244. https://doi.org/10.1007/s11676-018-0788-1
Yu DP, Wang QL, Wang GG, Dai LM (2006) Dendroclimatic response of *Picea jezoensis* along an altitudinal gradient in Changbai Mountains. Sci China 49:150–159. https://doi.org/10.1007/s11434-006-8116-0
Yu DP, Wang QW, Wang Y, Zhou WM, Ding H, Fang XM, Jiang SW, Dai LM (2011) Climatic effects on radial growth of major tree species on Changbai Mountain. Ann For Sci 68:921–933. https://doi.org/10.1007/s13595-011-0098-7
Yu DP, Liu JQ, Zhou L, Zhou WM, Fang XM, Wei YW, Jiang SW, Dai LM (2013) Spatial variation and temporal instability in the climate-growth relationship of Korean pine in the Changbai Mountain region of Northeast China. For Ecol Manage 300:96–105. https://doi.org/10.1016/j.foreco.2012.06.032
Yu J, Liu QJ, Zhou G, Meng SW, Zhou H, Xu ZZ, Shi JN, Du WX (2017) Response of radial growth of *Pinus koraiensis* and *Picea jezoensis* to climate change in Xiaoxing'anling Mountains, Northeast China. Chin J Appl Ecol 28:3451–3460. https://doi.org/10.13287/j.1001-9332.201711.008
Yu J, Lin WZ, Yan BQ (2018) Tree-ring reconstruction of June–August minimum temperature back to AD 1872 in Qinling Mountains, Northwest China. Quat Sci 38:971–980. https://doi.org/10.11928/j.issn.1001-7410.2018.04.15
Yu J, Chen JJ, Meng SW, Zhou H, Zhou G, Gao LS, Wang YP, Liu QJ (2021) Response of radial growth of *Pinus sylvestriformis* and *Picea jezoensis* to climate warming in the ecotone of Changbai Mountains, Northeast China. Chin J Appl Ecol 32:46–56. https://doi.org/10.13287/J.1001-9332.202101.004
Zhang XL, Bai XP, Chang YX, Chen ZJ (2016) Increased sensitivity of Dahurian larch radial growth to summer temperature with the rapid warming in Northeast China. Trees 30:1799–1806. https://doi.org/10.1007/s00468-016-1413-6
Zhang LN, Jiang Y, Zhao SD, Kang XY, Zhang WT, Liu T (2017) Lingering response of radial growth of *Picea crassifolia* to climate at different altitudes in the Qilian Mountains, Northwest China. Trees 31:455–465. https://doi.org/10.1007/s00468-016-1467-5
Zhang LN, Li SS, Hong YX, Zeng XM, Liu XH (2020a) Changes in the radial growth of *Picea crassifolia* and its driving factors in the mid-western Qilian Mountains, Northwest China since 1851 CE. Dendrochronologia 61:125707. https://doi.org/10.1016/j.dendro.2020.125707
Zhang Q, Yao YB, Li YH, Huang JP, Ma ZG, Wang ZL, Wang SP, Wang Y, Zhang Y (2020b) Causes and changes of drought in China: research progress and prospects. J Meteorol Res 34:460–481. https://doi.org/10.1007/s13351-020-9829-8
Zhang Y, Cao RJ, Yin J, Tian K, Xiao DR, Zhang WG, Yin DC (2020c) Radial growth response of major conifers to climate change on Haba Snow Mountain, Southwestern China. Dendrochronologia 60:125682. https://doi.org/10.1016/j.dendro.2020.125682
Zhou ZQ, Shi HY, Fu Q, Li TX, Gan TY, Liu SN, Liu K (2020) Is the cold region in Northeast China still getting warmer under climate change impact? Atmos Res 237:104864. https://doi.org/10.1016/j.atmosres.2020.104864
Zhu LJ, Li ZS, Zhang YD, Wang XC (2017) A 211-year growing season temperature reconstruction using tree-ring width in Zhangguangcai Mountains, Northeast China: linkages to the Pacific and Atlantic Oceans. Int J Climatol 37:3145–3153. https://doi.org/10.1002/joc.4906
Zhu LJ, Cooper DJ, Yang JW, Zhang X, Wang XC (2018) Rapid warming induces the contrasting growth of Yezo spruce (*Picea jezoensis* var. *microsperma*) at two elevation gradient sites of northeast China. Dendrochronologia 50:52–63. https://doi.org/10.1016/j.dendro.2018.05.002

Publisher's Note